Simulation of tubular reverse osmosis*

CJ Brouckaert and CA Buckley**
Pollution Research Group, Department of Chemical Engineering, University of Natal, King George V Avenue, Durban 4001, South Africa

Abstract

The rational design of reverse osmosis systems is made difficult because the engineering variables of pressure, flow rate, solute rejection and permeate flux are interrelated in a complex way, even before such effects as membrane fouling and degradation are taken into account. Where pilot-plant data may be available, unless they cover a very comprehensive range of operating conditions, it will still be difficult to estimate the consequences of varying the parameters in the process of seeking the most economic design. A similar situation applies to an existing plant which has to be adapted to changing circumstances.

Although complex, the underlying mechanisms of reverse osmosis are quite well understood, and are readily amenable to computer simulation. A computer package is being developed to serve as a tool for the analysis or design of reverse osmosis plants. Its use is demonstrated by means of a hypothetical case study based on pilot-plant data gathered at the Lethabo Power Station near Sasolburg.

Introduction

Reverse osmosis (RO) first became a commercially viable desalination process in the late 1960s, and rapidly established itself in the field of potable water production from brackish water, and later also from sea water. Today it is the preferred technology for these applications.

Almost from the beginning, the potential of RO for the treatment of industrial effluents and pollution control was recognised, since it provides a means for effecting a pure separation of solutes from water, with minimal or no addition of treatment chemicals, and with no phase change. Progress in this field has, however, not matched the spectacular achievements of the natural water desalination applications. Part of the reason for this is the sensitivity of RO membranes to fouling and chemical damage, together with the variability of industrial effluents, both from location to location, and with respect to time at a single location, so that the accumulation of relevant expertise is a relatively arduous process.

Commercial RO membranes are generally packaged in one of three major configurations: tubular, spiral-wrapped and hollow-fine-fibre modules. The latter two are very efficient in terms of providing a large surface area per unit volume, but are very sensitive to fouling, since mechanical cleaning of any sort is impossible. Tubular membranes typically have a 12,5 mm tube diameter, and are relatively tolerant of particulates in the feed, and can be cleaned by passing sponge-balls through them in addition to chemical cleaning methods. Thus, they may be the only practical choice for some effluents, in spite of their low capacity.

A computer model of tubular reverse osmosis (TRO) is being developed by the Pollution Research Group of the University of Natal, under the sponsorship of the Water Research Commission, as a tool to be used in the investigation, design and evaluation of aqueous effluent treatment plants, with special reference to the TRO modules manufactured by Membratek of Paarl.

In 1987 Eskom built a TRO plant to separate salts from the cooling tower blow-down at the Lethabo Power Station near Sasolburg. The motivation was to reduce the volume of saline effluent to that required for the conditioning of the station's ash dumps, thus achieving a zero aqueous effluent discharge to the environment. In the previous year, a pilot investigation was carried out using a plant consisting of 30 Membratek TRO modules, each containing 1,72 m² of cellulose-acetate membrane in 12,5 mm diameter tubes (Schutte et al., 1987). Eskom has made some of the data gathered from the pilot plant available to provide a realistic test of the modelling procedures.

This paper explores, through simulation, some aspects of the relationship between the pilot plant and the full-scale plant that was designed from it, to illustrate the use of computer modelling in conjunction with pilot-plant investigations.

Nomenclature

A = RO membrane pure water permeability coefficient, kg/m²
c = Solute concentration, kg/m³
d = Tube diameter, m
D = RO membrane solute transport coefficient, m/s
$\mathcal{D}$ = Molecular diffusivity of solute in water, m²/s
k = Turbulent diffusion mass transfer coefficient, m/s
L = Equivalent length of RO tube per module to account for pressure drops through fittings, m
N = Flux, kg/m²·s
P = Pressure, Pa
Q = Flow rate through RO tubes, m³/s
v = Flow velocity, m/s
ΔA = Incremental membrane area in numerical integration, m²
ΔL = Incremental tube length in numerical integration, m
ΔP = Incremental pressure drop in numerical integration, Pa
μ = Viscosity of water, Pa·s
Π = Osmotic pressure, Pa
ρ = Density of fluid, kg/m³
Sh = Sherwood number $\frac{kd}{\mathcal{D}}$

Re = Reynolds number $\frac{\rho v d}{\mu}$

Sc = Schmidt number $\frac{\mu}{\rho \mathcal{D}}$

Subscripts

b = In the bulk solution within an RO tube
m = In the solution at the membrane surface

*Revised paper. Originally presented at the 6th National Meeting of the South African Institution of Chemical Engineers, Elangeni Hotel, Durban, South Africa, 7 to 9 August 1991.
**To whom all correspondence should be addressed.
Received 28 January 1992; accepted in revised form 21 April 1992.

p = In the RO permeate
s = Solute
w = Water

The basis of the computer model

There are two major theories of transport through RO membranes in the literature, the so-called solution-diffusion model, and the finely-porous-capillary model (Rautenbach and Albrecht, 1989). The latter model is largely due to the work of Sourirajan and co-workers over the last 30 years (Sourirajan and Matsuura, 1985). It has been shown (Muldowney and Punzi, 1988) that the predictions of the two models are virtually identical in practice. The formulation used in this work is based on the one due to Sourirajan.

The conceptual basis of the model is illustrated in Fig. 1.

Water is driven through the membrane by the pressure gradient. As the solute is rejected by the membrane, it is concentrated in a layer adjacent to the membrane surface. This raises the osmotic pressure, Π_m, of the solution at this point. The concentrating tendency is limited by turbulent diffusion of the solute back into the bulk flow. The flux of water N_w through the membrane is taken as proportional to the difference in the effective pressure (P - Π) across the membrane:

$$N_w = \frac{A}{\mu} [(P_m - \Pi_m) - (P_p - \Pi_p)]$$

where:

A is a constant, characteristic of the membrane
μ is the viscosity of water
P is the piezometric pressure
Π is the osmotic pressure of the solution
subscripts m and p refer to positions at the inner and outer membrane surfaces respectively.

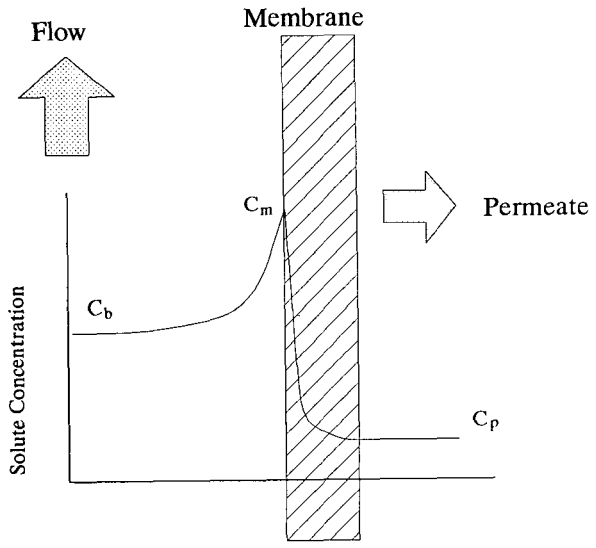

Figure 1
A schematic diagram of the reverse osmosis model. The solute concentration increases from c_b in the bulk solution to c_m adjacent to the membrane, and then decreases through the membrane to c_p in the permeate.

Although the solute is rejected by the membrane, some does diffuse through. The solute flux N_s is given by:

$$N_s = D (c_m - c_p) \quad (2)$$

Here D is a transport coefficient which is dependent on the membrane material, its effective thickness, and nature of the solute; and c_m and c_p are the solute concentrations at the inner and outer membrane surfaces respectively.

Finally, the concentration at the inner membrane surface, c_m, is determined by a balance between the convective transport of solute towards the membrane by the water flux, and the opposing turbulent diffusion of solute away from the surface. Standard film-diffusion theory yields the relationship:

$$N_w = k (1 - c_p) \ln \left[\frac{c_m - c_p}{c_b - c_p} \right]$$

where:
N_w is the flux of water through the boundary layer film, and k is a turbulent mass transfer coefficient, the magnitude of which is related to the Reynolds number of the flow in the tube. At steady state the flux through the boundary layer is the same as the flux through the membrane.

Simultaneous solution of these three equations yields the water and solute fluxes at any point in the TRO train. To calculate the performance of the whole system, these point predictions must be integrated down the length of the tubes, taking into account the changing pressure, flow rate and concentrations as the RO process takes place. Further details of the numerical procedures appear in the Appendix.

The adjustable parameters in this scheme are the constants A and D, which depend on the membrane and the solute involved. The turbulent mass transfer coefficient, k, can be determined from literature correlations. The correlation used in this study was (Belfort, 1984):

$$Sh = 0{,}0096 \cdot Re^{0{,}913}\, Sc^{0{,}346}$$

where:
Sh is the Sherwood number,
Re is the Reynolds number, and
Sc is the Schmidt number

The Lethabo TRO pilot-scale and full-scale plants

The Lethabo pilot-scale and full-scale plants have been described by Schutte et al. (1987). The pilot plant consisted of three banks of TRO modules. The first bank contained three parallel rows of four modules in series, the second bank 2 x 4, and the third 1 x 10 (see Fig. 6b). This tapered configuration was aimed at maintaining the flow velocities in the tubes as the overall volumetric flow rate progressively decreased down the tubes. The full-scale plant does not make use of a tapered configuration; it consists of 5 184 modules in essentially a 432 x 12 array, although they are physically organised in smaller blocks.

The pilot-plant data, which Eskom made available for this study, consisted mainly of pressures, flow rates and conductivities measured on the feed, permeate and concentrate streams. In addition a limited number of detailed chemical analyses were performed on samples of these streams. A representative set of analyses appears in Table 1.

TABLE 1
TYPICAL ANALYSES OF PILOT-PLANT STREAMS

Determinand		Feed	Permeate	Concentrate
Cl^-	mg/ℓ	270	45,8	650
SO_4^{2-}	mg/ℓ	1 140	54,5	2 491
Ca^{2+}	mg/ℓ as $CaCO_3$	425	2,8	1 078
Mg^{2+}	mg/ℓ as $CaCO_3$	90	1,2	214
Na^+	mg/ℓ	406	47	956
K^+	mg/ℓ	76	3,3	250
PO_4^{3-}	mg/ℓ	0,48	0,02	0,73
SiO_2	mg/ℓ	39,3	14,8	82,7
Conductivity	mS/m	313	27	722
pH		5,5	5,5	5,9

TABLE 2
PILOT-PLANT OPERATING CONDITIONS SELECTED FOR MODEL PARAMETER DETERMINATION

Model parameters		Measured	Simulation
A	kg/m^2	-	$2,21 \times 10^{-6}$
D	m/s	-	$2,01 \times 10^{-6}$
L	m	-	0,11
Input variables			
Temperature	°C	27	27
Feed pressure	MPa	2,9	2,9
Feed flow rate	m^3/h	1,46	1,46
Feed conductivity	mS/m	370	370
Output variables			
Exit pressure	MPa	1,9	1,82
Permeate flow rate	m^3/s	1,05	1,06
Permeate conductivity	mS/m	27	25

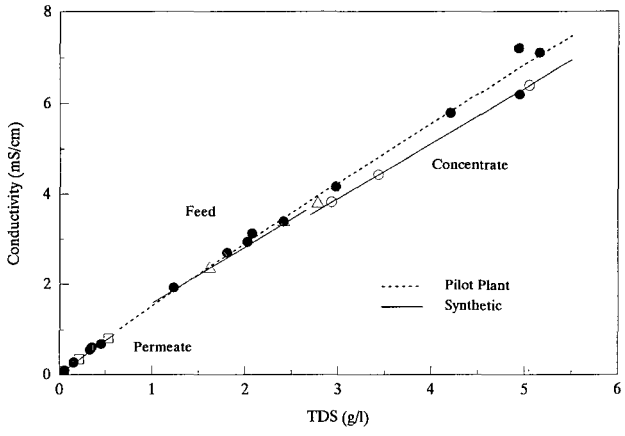

Figure 2
The relationship between TDS and conductivity for the Lethabo pilot plant streams. Representative data from the pilot plant feed, permeate and concentrate streams are compared with synthetic solutions based on the analyses shown in Table 1.

In its present stage of development, the model only allows for a single solute. Furthermore it requires, as data, a relationship between solute concentration and osmotic pressure, a quantity which had not been measured by Eskom. It was decided to use total dissolved solids (TDS) as a single pseudo-solute, and to determine relationships between TDS, conductivity and osmotic pressure from synthetic solutions, made up in the laboratory to match the Eskom analyses. Since the different ionic species are rejected to different extents by the RO membranes (for instance, divalent ions tend to be more strongly rejected than monovalent ions) the relative proportions of the ions differ in the feed, permeate and concentrate streams. Thus there were potentially three sets of these relationships for the three streams. Three stock solutions were made up to match the relative salt concentrations shown in Table 1, and then three solutions were made from each of these by dilution.

Figures 2 and 3 show the results of these measurements. The data are satisfactorily represented by a single set of relationships. In the case of the conductivities, the values reported in the Eskom analyses could be compared with those determined for the synthetic solutions: the correspondence shown in Fig. 2 is quite satisfactory.

The relationships used for the model were obtained from the data by simple linear regression:

$$\textit{Conductivity}\ (mS/m) = 1{,}391 \times 10^2 \times \textit{TDS}\ (g/\ell) \qquad (5)$$

$$\textit{Osmotic pressure}\ (kPa) = 43{,}55 \times \textit{TDS}\ (g/\ell) \qquad (6)$$

The simple relationships that were found seem to justify to some extent the approximations involved in representing the mixed solute as a single entity.

Equations (5) and (6) represent the physical chemistry of the solutions for modelling purposes. The remaining modelling parameters needed to be obtained from the pilot-plant performance data. These were the membrane parameters, A and D in Eqs. (1) and (2), and an additional parameter representing the hydraulic pressure drops across the module array.

The pressure drop in the RO tubes is calculated according to the standard friction factor correlation for turbulent flow in pipes; however, additional pressure drop is incurred by the u-bend connectors between tubes within the modules, and the inter-connectors and manifolds between the modules. These were modelled simply as an extra length L of (impermeable) tube for each RO tube in each module. Simulations of the pilot-plant configuration were run for a specific feed pressure, flow rate and conductivity, and the values of A, D and L adjusted to fit the permeate flow rate and conductivity, and the concentrate exit pressure.

The available pilot-plant data covered nine months of operation, during which time the membranes went through a number of cycles of progressive fouling, followed by cleaning, possibly with longer term irreversible deterioration also taking place. One would expect to find the modelling parameters to be correlated with the varying condition of the modules, and it would be very interesting to subject the data to such an analysis. For the purpose of this paper, however, a single set of parameters was chosen corresponding to conditions just after the membranes had been cleaned, as summarised in Table 2.

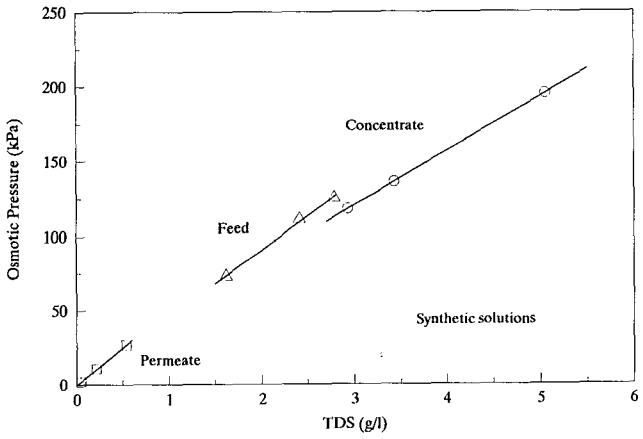

Figure 3
The relationship between TDS and osmotic pressure for the Lethabo pilot plant streams. Measurements on synthetic solutions are based on the analyses shown in Table 1.

Simulations of the full-scale plant configuration

As mentioned above, the full-scale plant consists of 432 parallel rows of 12 modules in series. Schutte et al. (1987) presented a set of operating conditions, from which the following figures (Table 3) have been extracted:

TABLE 3
OPERATING CONDITIONS FOR FULL-SCALE PLANT

		Feed	Permeate	Concentrate
Flow	m³/h	375	263	112
TDS	mg/ℓ	1 300	81	4 276
Temperature	°C	25-30		

Unfortunately no operating pressure was reported, so a complete comparison between plant data and the simulation was not possible. For feed conditions as in Table 2, and a feed pressure of 4 MPa, the model gave the following results (Table 4):

TABLE 4
SIMULATED PERFORMANCE OF THE LETHABO PLANT AT 4 MPa

		Permeate	Concentrate
Flow	m³/h	268	107
TDS	mg/ℓ	60	4 400

The agreement is sufficiently good to show that the simulation is reasonably realistic, which is all that is required for the purpose of this paper.

(a)
Effective pressure driving force for water permeation (total pressure - osmotic pressure) across the membrane at the plant exits. Hydraulic pressure drop prevents the pilot plant from being operated at water recoveries below about 50%.

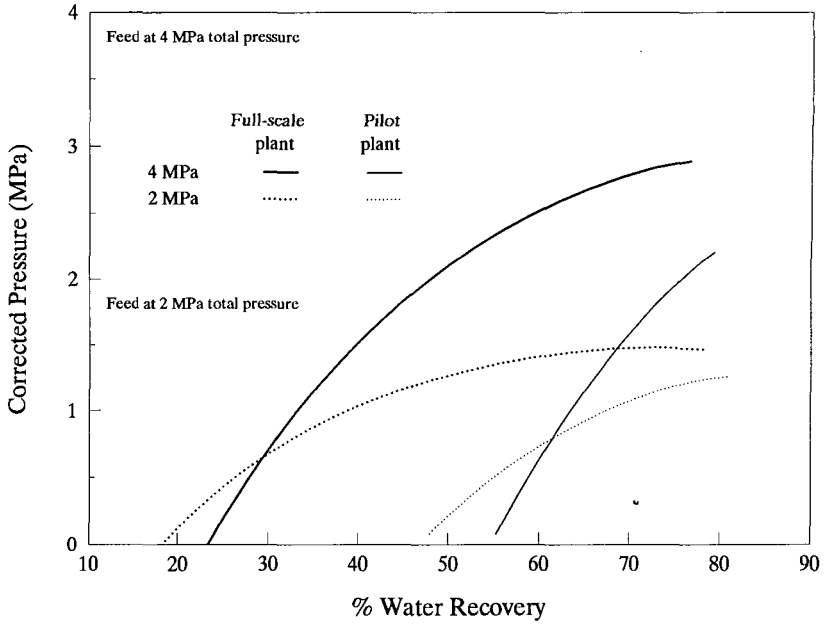

(b)
Total dissolved solids in the permeate stream.

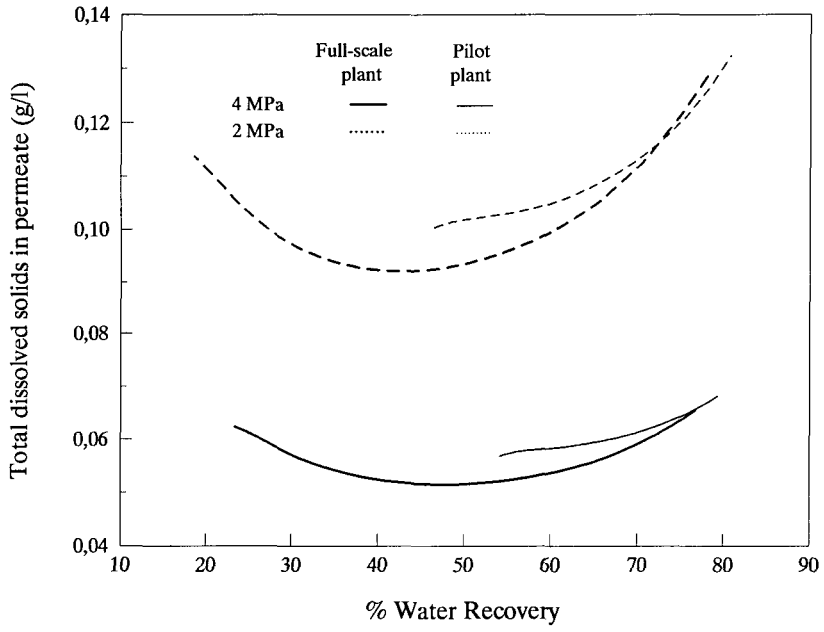

Figure 4
Simulated results for the Lethabo pilot plant and full-scale plant at feed pressures of 2 MPa and 4 MPa.

Comparison between the pilot-plant and full-scale plant configurations

A pilot study is undertaken in order to obtain data on which to base the eventual design of the plant. This data includes the relationships between equipment performance measures, such as flux and rejection, and operating parameters, such as pressure, flow rate and water recovery, as well as safe operating limits, and some assessment of the requirements for maintenance procedures such as membrane cleaning and membrane replacement.

Given the complex interdependence of variables in RO equipment, there is an interesting question as to what the relationship is between measurements made in the pilot plant and the equivalent variables for the full-scale configuration. This question is, of course, a crucial one for the engineer who bases his design on the pilot-plant data. Simulation provides a convenient method for investigating such questions, given that the model is reasonably realistic.

Figures 4 to 6 show the results of a set of comparative simulations for the Lethabo pilot plant and full-scale plant configurations. For all simulations feed conditions of 1 300 g/ℓ TDS and 27°C were used. Two feed pressures were investigated,

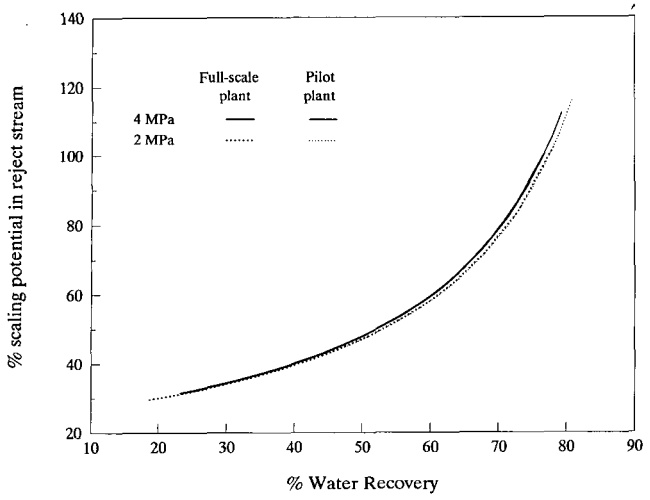

Figure 5
Solute concentrations in the concentrated brine streams of the Lethabo pilot plant and full-scale plant, expressed in terms of $CaSO_4.2H_2O$ scaling potential.

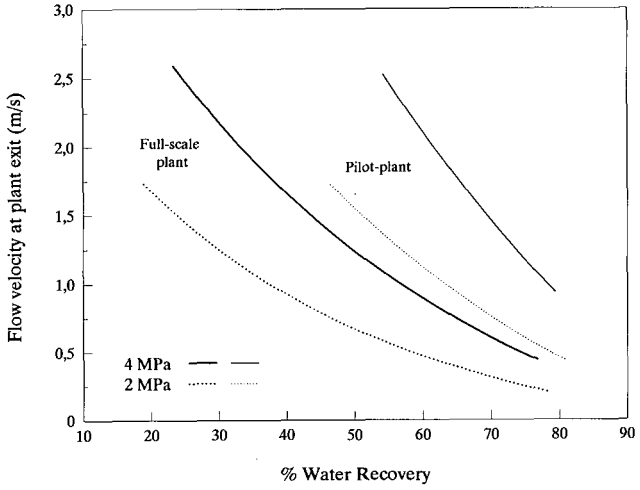

Figure 6
Simulated results for the Lethabo pilot plant and full-scale plant at feed pressures of 2 MPa and 4 MPa.
a) Flow velocities in the concentrated brine streams at the plant exits.

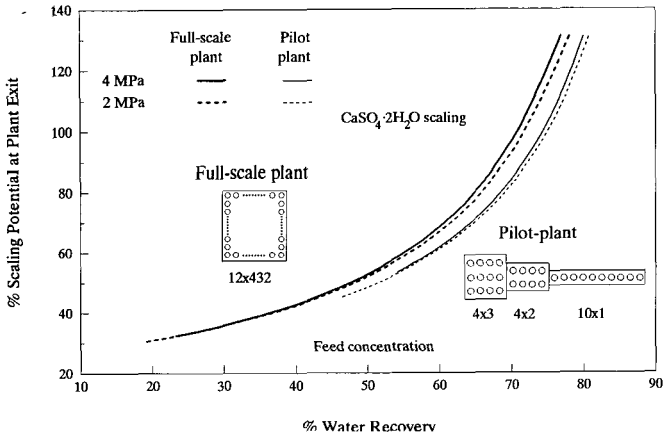

b) Solute concentrations in the boundary layer adjacent to the membrane surface at the plant exits, expressed in terms of $CaSO_4.2H_2O$ scaling potential.

2 MPa and 4 MPa and appropriate feed flow rate ranges for each configuration. In order to allow direct comparison of the two configurations, the results are presented in terms of water recovery and pressure. Since the permeate flow rate is largely determined by the pressure, for a given pressure there is an inverse relationship between water recovery and feed flow rate.

The first point of difference between the two configurations is that the full-scale configuration can be operated over a considerably wider range of water recoveries than the pilot plant. This is because the latter has a greater number of modules in series, as well as a tapered configuration, which leads to a higher hydraulic pressure drop. The lower limit for water recovery corresponds to the situation where the outlet pressure drops to atmospheric pressure. Naturally this would not be a practical operating condition as the flux through the later modules in the train would be much reduced. The driving force for permeation is the hydraulic pressure difference minus the osmotic pressure difference across the membrane; its value at the plant exit for the two configurations is shown in Fig. 4a.

The behaviour of the permeate quality, shown in Fig. 4b, is very interesting. For the full-scale configuration it passes through a minimum at 40 to 50% water recovery. The water is driven through the membrane by pressure, whereas the solute passes through by a concentration gradient driven diffusion. At higher water recoveries, the permeate concentration increases due to the higher concentration in the tubes, whereas at lower water recoveries, the increase is due to the lower water flux as a result of the reduced average pressure caused by the high flow rate. In the case of the pilot plant, the pressure drop limit is reached before the minimum occurs.

As can be seen from Fig. 5, the reject concentration is almost entirely determined by water recovery, and is very little dependent on pressure or configuration. One of the reasons that the reject concentration is of interest is that salts in the solution may be concentrated above their saturation limit, and cause scaling of the equipment. The critical component of the Lethabo effluent in this regard is gypsum ($CaSO_4.2H_2O$). For the feed composition shown in Table 1, it was calculated from solubility data quoted in Rautenbach and Albrecht (1989) that gypsum exceeds its solubility limit at a TDS of 5,2 g/ℓ. The concentration is expressed as a per cent scaling potential in Fig. 5 by taking 5,2 g/ℓ as 100%. This occurs at a water recovery of about 75%, which may be compared with the Lethabo plant operating figure of 70% quoted by Schutte et al. (1987). It is interesting that the pilot plant was initially operated at 76% water recovery, but this was later dropped to 70% after scaling problems were encountered, and the latter value was chosen for the full-scale plant design.

If one considers the diagram in Fig. 1, the reject concentration corresponds to the bulk concentration at the plant exit, c_b. It is clear that this is not the highest concentration that the membranes encounter; instead the highest concentration is in the boundary layer immediately adjacent to the membrane surface, c_m. This concentration is not easily observable in an experimental sense; however, it is a key variable in the model. From Fig. 6a it can be seen that the pilot-plant configuration generates higher flow velocities at the exit, which lead to high turbulent mass transfer, and a lower concentration rise in the boundary layer.

Figure 6b shows the variation of c_m at the plant exits, once again expressed as per cent scaling potential. It can be seen that, for the feed conditions chosen, the full-scale plant is appreciably more prone to scaling than the pilot plant. In particular, at 70% water recovery the pilot plant is in a non-scaling region, whereas

the full-scale plant is in a scaling region. The steepness of the curves at this point indicates that the situation would be very sensitive to changes in conditions, such as an increase in feed concentration.

The effect of operating variables on the performance of the Lethabo full-scale plant

A set of simulations was run for the following feed conditions:

Pressure	: 2,5 to 4,5 MPa
Flow	: 250 to 450 m³/h
TDS	: 1 300 mg/ℓ
Temperature	: 27°C

It turned out that not all these combinations of pressure and flow gave feasible solutions: at high pressures and low flows the tubes ran dry before the exit was reached. In practice, a limit would be reached even sooner than the model indicated, because of precipitation of scale on the membranes. As previously discussed, the TDS value at which $CaSO_4.2H_2O$ would start to precipitate was taken as 5,2 g/ℓ.

Figure 7 shows the response surface for the membrane concentration, with the scaling limit contour plotted. Since this contour represents an important limitation on the plant's operation, it has been transferred to some of the other response surface plots for reference.

Figure 8 shows the corresponding plot for the solute concentration in the concentrate stream. It can be seen that the scaling limit on the membranes occurs before the solubility product is exceeded in the concentrate.

Figures 9 and 10 are the corresponding response surfaces for the permeate flux and concentration. Note that the viewing orientations have been changed from the other plots in order to get a better impression of the surface shapes.

Optimising a design according to some economic objective is a standard design technique. Ideally this objective function should include contributions for capital costs, running costs, maintenance etc. Since the purpose of this paper is only to illustrate a methodology, a simplified objective function is presented in Fig. 11.

The purpose of the plant is to remove salt from the cooling tower circuit, while replacing the water. The benefit, therefore, can be expressed as the mass of salt removed from the permeate, calculated as:

Permeate flow × (Feed TDS - Permeate TDS)

The power cost incurred is simply *pressure × flow rate* for the feed.

The ratio of these quantities can be termed the plant productivity expressed as kg salt removed per MJ of energy expended.

Figure 11 shows the plot for productivity, thus defined. It can be seen how the productivity is favoured by high pressures and low flow rates, and how it is limited by membrane scaling.

It is worth noting that the benefits of such an optimisation could not be realised by adjusting the pressure and flow after the plant was built, because reducing the feed pressure to the plant by throttling the pumps would not reduce their power consumption.

Finally, Fig. 12 shows the productivity surface for a different configuration of 5 184 modules, consisting of 8 rows of 432 modules, followed by 8 rows of 216 modules - a tapered

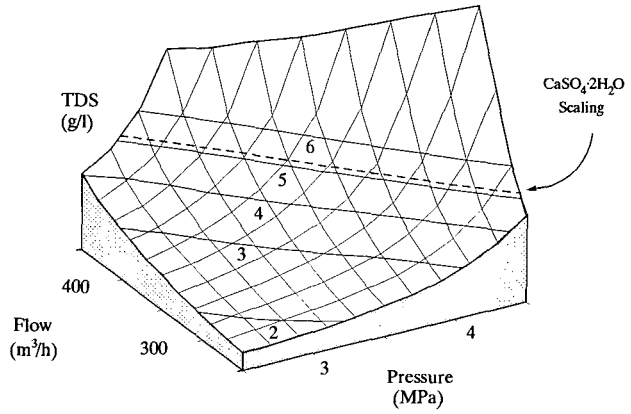

Figure 7
Simulated response surface for membrane concentration for the full-scale Lethabo TRO plant. The broken line indicates the limiting locus of conditions which will result in gypsum starting to precipitate on the membrane surfaces at the plant exit.

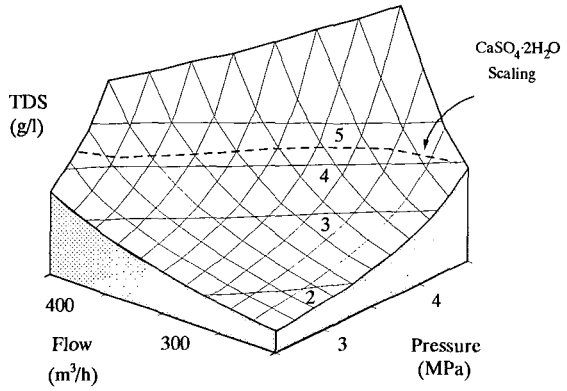

Figure 8
Simulated response surface for exit concentration for the full-scale Lethabo TRO plant to feed pressure and flow rate. The broken line indicates the limiting locus of conditions which will result in gypsum starting to precipitate on the membrane surfaces at the plant exit.

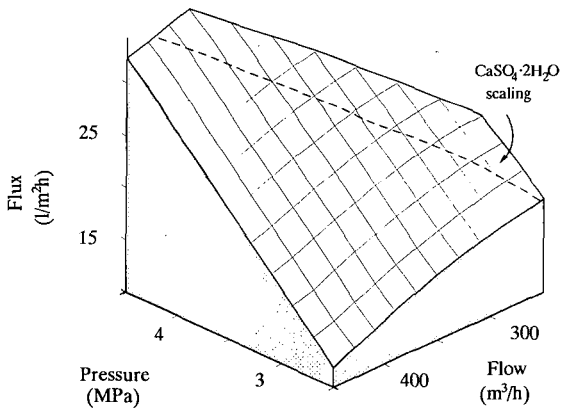

Figure 9
Simulated response surface for permeate flux of the full-scale Lethabo TRO plant to feed pressure and flow rate.

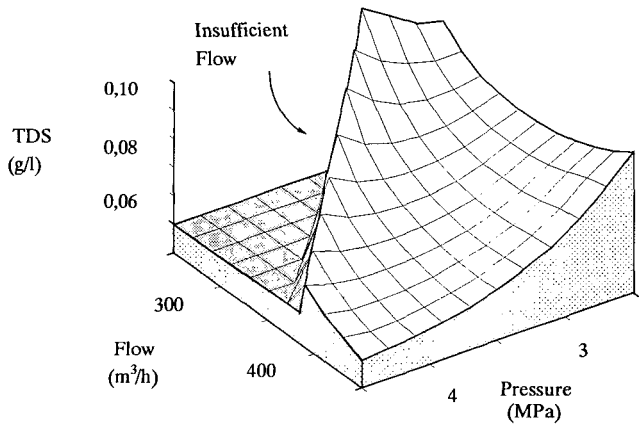

Figure 10
Simulated response surface of permeate concentration of the full-scale Lethabo TRO plant to feed pressure and flow rate. At the higher pressures the lower feed flow rates are insufficient to maintain a reject stream flow at the plant outlet.

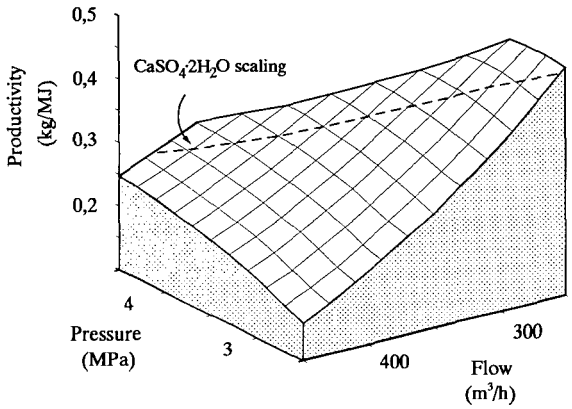

Figure 11
Simulated response surface of the productivity of the full-scale Lethabo TRO plant to feed pressure and flow rate.

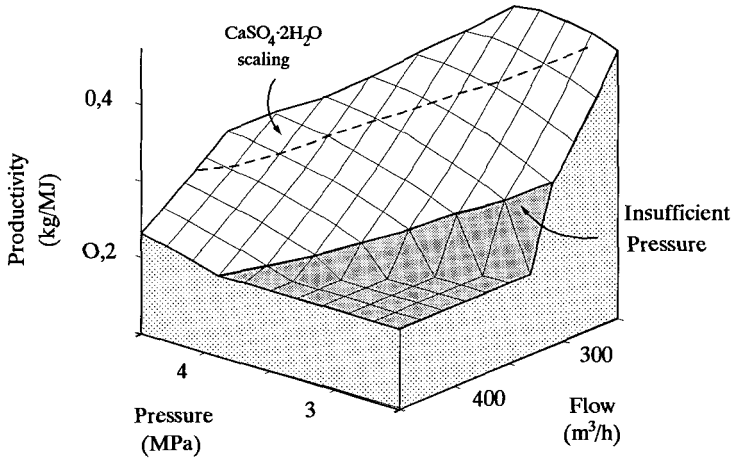

Figure 12
Simulated response surface for the productivity of a tapered-configuration TRO plant, equivalent in size to the full-scale Lethabo TRO plant, to feed pressure and flow rate. At the higher flow rates the lower pressures are insufficient to overcome the hydraulic resistance of the plant.

configuration. It can be seen that the productivities of this latter configuration are much the same as for the former, but that a new constraint appears, in that the lower pressures are not able to achieve some of the higher flow rates through the plant. As might be expected, the $CaSO_4.2H_2O$ scaling is slightly less restricting, because of the higher flow velocities at the back-end of the plant. This alternative configuration is not proposed here as being superior to the original, but is included to illustrate the point that having a model available would allow a designer to explore the characteristics of alternative configurations in order to choose the optimum one.

Conclusions

This study has shown that the model, even in its present relatively simple form, is able to represent the performance of a real plant to a useful degree of accuracy, and should be able to enhance the quality of information obtained from pilot-plant work, by allowing investigators to explore the implications that their findings hold for the eventual design.

Since only a limited amount of the pilot plant data was used in determining the simulation parameters, important considerations such as membrane fouling, cleaning and degradation, as well as variations in feed quality, are not reflected in the simulations that have been presented. Consequently the results should not be seen as constituting a commentary on the actual design of the Lethabo plant.

Acknowledgements

The authors wish to acknowledge the contributions of Eskom and Miss BM Brouckaert for the laboratory work and the preparation of the diagrams. This investigation was undertaken in terms of a Water Research Commission project.

References

BELFORT, G (1984) *Synthetic Membrane Processes.* Orlando: Academic Press.

MULDOWNEY, GP and PUNZI, VL (1988) A comparison of the solute rejection models in reverse osmosis membranes. System : Water-sodium chloride-cellulose acetate. *Ind. Eng. Chem. Process Res. Dev.* **27** 2341.

PERRY, JH (1963) *Chemical Engineers' Handbook.* McGraw-Hill, Tokyo.

RAUTENBACH, R and ALBRECHT, R (1989) *Membrane Processes.* Chichester : John Wiley and Sons.

SCHUTTE, CF, SPENCER, T, ASPDEN, JD and HANEKOM, D (1987) Desalination and re-use of power plant effluents from pilot plant to full-scale application. *Desalination* **67** 255-269.

SOURIRAJAN, S and MATSUURA, T (1985) *Reverse Osmosis/Ultrafiltration Process Principles.* Ottawa: National Research Council, Canada.

Appendix 1

Description of the tubular reverse osmosis model algorithm

The transport of water and solute through the TRO membrane at any point is governed by Eqs. (1), (2) and (3), the membrane parameters A and D, and the local values of the variables P, c_b and k. A standard modelling situation is considered, in which A and D are known, as are P, c_d and Q, the flow rate for the feed stream. Thus the transport equations can be solved at the entrance to the plant, to yield permeate flux and concentration.

From a material balance and hydraulic pressure drop calculation, the change in the conditions of the solution flowing in the tubes may be calculated as it passes through a length of the tubes, ΔL. Repeated application of this procedure constitutes an Euler method numerical integration of the whole process along the length of the tubes.

Solution of the transport equations at a point

The numerical solution of the transport equations is considered in some detail by Sourirajan and Matsuura (1985), and their method was followed in this work, with some modifications. In the standard modelling situation, the three equations contain four unknowns, N_s, N_w, c_b and c_p.

The material balance on the solute:

$$c_p = \frac{N_s}{N_w + N_s}$$

completes the description of the process. Since the equations are non-linear and require numerical solution, it is advantageous to reduce as much as possible the number of equations that must be solved simultaneously. By combining the four equations, it is possible to reduce them to two equations involving c_m and c_p. Various combinations are possible, and the one chosen here was:

$$A[P - \Pi_m + \Pi_p]c_p - D(1 - c_p)(c_m - c_p) = 0$$

$$c_m - c_p - (c_b - c_p) \exp\left[\frac{D(c_m - c_p)}{kc_p}\right] = 0$$

This choice was different to the one adopted by Sourirajan and Matsuura, and was selected because it led to an algorithm that was less likely to cause computer arithmetic errors (numerical overflow or division by zero) when the numerical solution procedure tried unrealistic values for c_m and c_p. The above two equations were solved using a standard Newton-Raphson method.

Hydraulic modelling

Where the flow was divided between parallel rows of modules, it was assumed that the division was even. For the Euler integration, the step ΔL was taken as the length of one tube in the module (2,3 m). The pressure drop down the tube was calculated using the Blasius formula (Perry, 1963) for smooth pipes:

$$\frac{\Delta P}{\Delta L} = -0{,}079 \cdot \left(\frac{\rho v^2}{d}\right) \cdot Re^{-0{,}25}$$

An extra pressure drop corresponding to the extra and equivalent

length of the hydraulic fitting and returned bends was added for each tube.

Material balance

After the transport equations had been solved in each step of the integration, the flows and concentrations on either side of the membrane were updated according to the quantities of water and solute transferred.

Thus, considering the i th incremental section of RO tube, with membrane area, ΔA:

$$Q^i = Q^{i-1} - (N_w^i + N_s^i)\ \Delta A$$

$$c_b^i = \frac{c_b^{i-1} Q^{i-1} - c_p^i (N_w^i + N_s^i)}{Q^i}$$

Since a single permeate stream was produced by the plant, it was a mixture of the permeates produced by each RO tube in the plant. Its flow and composition was calculated as:

$$Q_p = \sum_i (N_w^i + N_s^i)$$

$$c_p = \frac{\sum_i N_s^i}{Q_p}$$